

## 质谱学报

Journal of Chinese Mass Spectrometry Society

# 水相中酒石酸铀酰形态的电喷雾串联质谱研究

曾 凯<sup>1,2</sup>, 陈焕文<sup>1</sup>, 罗明标<sup>1</sup>, 张 慧<sup>1</sup>, 余文婷<sup>1</sup>, 杨亚宣<sup>1</sup>

(1. 东华理工大学, 江西省质谱科学与仪器重点实验室, 江西 南昌 330013;

2. 南昌市食品药品检验所, 南昌市中药质量控制与安全性评价重点实验室, 江西 南昌 330012)

**摘要:** 铀的水溶液化学形态是高放废物处置研究的重要内容之一。本实验采用电喷雾串联质谱(ESI-MS/MS)研究酒石酸-硝酸铀酰水溶液中铀酰形态, 共分析出14种酒石酸铀酰和5种无机铀酰形态。每个铀酰基团可紧密结合1个酒石酸阴离子, 并继续以较弱的形式络合1~2个酒石酸分子。实验中还发现了 $[(\text{UO}_2 \text{HTarH}_2 \text{Tar})_2]^{2+}$ 、 $[(\text{UO}_2)_3 \text{Tar}(\text{HTar})_2 (\text{H}_2 \text{Tar})_2]^{2+}$ 等酒石酸铀酰团簇形态。酒石酸铀酰形态中各络合键解离所需能量大小顺序为: 铼酰间结合键>酒石酸阴离子-铀酰结合键>酒石酸分子-铀酰结合键。该研究对实际条件下铀与有机酸的水溶液形态研究具有指导意义。

**关键词:** 电喷雾串联质谱(ESI-MS/MS); 铼形态; 酒石酸铀酰; 铼酰离子( $[\text{UO}_2]^{2+}$ )

**中图分类号:** O657.63      **文献标志码:** A

**doi:** 10.7538/zpxb.2018.0117

## Study of Uranyl Tartrate Speciation in Aqueous Solution by Electrospray Ionization Tandem Mass Spectrometry

ZENG Kai<sup>1,2</sup>, CHEN Huan-wen<sup>1</sup>, LUO Ming-biao<sup>1</sup>, ZHANG hui<sup>1</sup>,  
YU Wen-ting<sup>1</sup>, YANG Ya-xuan<sup>1</sup>

(1. Jiangxi Key Laboratory for Mass Spectrometry and Instrumentation,

East China University of Technology, Nanchang 330013, China;

2. Nanchang Key Laboratory of Quality and Safety Evaluation of Traditional Chinese Medicine,

Nanchang Institute for Food and Drug Control, Nanchang 330012, China)

**Abstract:** As a nuclear fuel, uranium plays an important role in national defense and energy, however, the release of uranium into the natural environment from mining to radioactive waste disposal poses a severe threat to public health and environmental protection. Therefore, investigation of uranium in aqueous solution is one of the important research on geological disposal of high level waste. Electrospray ionization tandem mass spectrometry (ESI-MS/MS) has been applied for trace detection of uranyl complex in the last decade because of its characteristics of accurate qualitative and quantitative capa-

收稿日期: 2018-09-12; 修回日期: 2018-11-24

基金项目: 国家自然科学基金(21761001); 长江学者和创新团队发展计划(IRT13054); 东华理工大学研究生创新基金(YC2017-B082)资助

作者简介: 曾 凯(1983—), 男(汉族), 江西吉安人, 高级工程师, 从事质谱分析研究。E-mail: 89692176@qq.com

通信作者: 罗明标(1963—), 男(汉族), 湖南益阳人, 教授, 从事分析化学研究。E-mail: luomingbiao\_ecut@126.com

bility, strong anti-interference capability and high determination efficiency. In this work, uranyl complex were identified by ESI-MS/MS, where the cations were ionized by ESI, positive charged uranyl tartrate undergoes characteristic fragmentation in the gas phase. Target ions were bombarded to generate product ions at high collision energy of 200 V in collision-induced dissociation (CID) mode, energy of which is far beyond normal range. As  $[\text{UO}_2]^+$  has special mass-to-charge ratio ( $m/z$ ) compared with other substances and it was split apart hardly, product ion of  $[\text{UO}_2]^+$  ( $m/z$  269.9) was the key basis to identify uranium-containing species in ESI-MS/MS. Pretreatment was unessential for the qualitative method which would not change speciation of original solution. It was found 14 kinds of uranyl tartrate and 5 kinds of inorganic uranyl speciation quickly in uranyl nitrate-tartaric acid solution, all of which could generate  $[\text{UO}_2]^+$  signal significantly or even uniquely. Each uranyl group could bind a tartrate anion tightly and was able to complex two tartaric acid molecular maximum. Experiment results showed that clusters of uranyl tartrate such as  $[(\text{UO}_2\text{HTarH}_2\text{Tar})_2]^{2+}$  and  $[(\text{UO}_2)_3\text{Tar}(\text{HTar})_2(\text{H}_2\text{Tar})_2]^{2+}$  were identified by ESI-MS/MS for the first time. Despite of losing the acid molecules, there was other mass fragmentation path of uranyl tartrate cluster ions that stable double bonds were reconstructed in the form of tartaric acid groups of the ions dehydrated. Moreover, the cleavage energy of uranyl tartrate complex bond was sorted in the following order: tartrate uranyl clusters bond energy > tartrate anion-uranyl bond energy > tartrate acid molecule-uranyl bond energy. The study indicates that ESI-MS/MS method has promising perspectives for the exploration of aqueous speciation of uranium with organic acids for environmental sample, and has guiding significance for speciation analysis of other lanthanide elements.

**Key words:** electrospray ionization tandem mass spectrometry (ESI-MS/MS); uranium speciation; uranyl tartrate; uranyl ion( $[\text{UO}_2]^+$ )

铀在国防、能源等领域具有重要作用<sup>[1]</sup>，但从铀的开采<sup>[2-4]</sup>到放射性废物处置过程<sup>[5-7]</sup>都可能对生态环境造成影响或伤害，而铀形态对铀的环境迁移特性及生物毒性有重要影响<sup>[8-12]</sup>。潘自强、钱七虎院士指出：铀等关键核素的水溶液化学形态与酒石酸等有机酸络合行为是处置化学须重点研究的内容之一<sup>[13]</sup>。研究铀与有机酸的结合形态，对完善铀污染治理方法，以及阐述铀的地球化学循环具有重要意义<sup>[14-20]</sup>。

电喷雾串联质谱(ESI-MS/MS)具有无需样品前处理、不改变样品原有形态、定性定量结果准确、抗干扰能力强、测定高效等特点，现已逐渐成为结构、形态研究的重要手段之一<sup>[21]</sup>。2003年，Pasilis等<sup>[22]</sup>首先将电喷雾质谱用于柠檬酸铀酰溶液形态研究，并将结果与拉曼、红外等传统分析方法的结果进行对比验证。2009年，Tserkezos等<sup>[23]</sup>证明了ESI-MS/MS定性

研究硝酸铀酰水溶液形态的准确性。之后的近10年内，电喷雾质谱越来越广泛地应用于含铀化合物的研究<sup>[24-30]</sup>。

本研究拟采用电喷雾离子源-三重四极杆串联质谱，利用铀酰基团( $^{[238}\text{UO}_2]^+$ )解离能远超一般有机小分子的特点，通过质谱碰撞池中的中性氮气分子高能碰撞诱导解离(CID)快速鉴别含铀化合物，对酒石酸铀酰络合形态进行快速鉴别和表征，获得水溶液中酒石酸铀酰络合物形态及其质谱裂解规律，为深入探索核素与有机酸的水溶液形态研究提供方法支持。

## 1 实验部分

### 1.1 主要仪器与装置

G6460三重四极杆串联质谱仪：美国Agilent公司产品，配有电喷雾离子源及MassHunter 6.0

数据处理系统;XS205 十万分之一天平:瑞士 Mettler Toledo 公司产品。

## 1.2 主要材料与试剂

六水合硝酸铀酰( $\text{UO}_2(\text{NO}_3)_2 \cdot 6\text{H}_2\text{O}$ ):纯度 $\geqslant 99.0\%$ ,湖北楚盛威化工有限公司产品;酒石酸( $\text{H}_2\text{Tar}$ ):纯度 $\geqslant 99.8\%$ ,国药集团化学试剂有限公司产品;实验用水为超纯水。

## 1.3 实验条件

ESI 正离子模式;进样流速: $10\ \mu\text{L}/\text{min}$ ;扫描范围: $m/z 220\sim 2\ 000$ ;碎裂电压: $90\ \text{V}$ ;加速电压: $7\ \text{V}$ ;毛细管电压: $4\ 500\ \text{V}$ ;干燥气:温度 $300\ ^\circ\text{C}$ ,流速 $11\ \text{L}/\text{min}$ ;雾化器压力: $103.4\ \text{kPa}$ ;四极杆温度: $100\ ^\circ\text{C}$ ;真空度: $2.8 \times 10^{-3}\ \text{Pa}$ 。

## 1.4 样品溶液制备

精密称取 $1.048\ 6\ \text{g}$ 酒石酸于 $500\ \text{mL}$ 容量瓶中,用纯水定容,得 $0.010\ \text{mol/L}$ 酒石酸溶液;称取 $1.237\ 2\ \text{g}$ 六水合硝酸铀酰于 $250\ \text{mL}$ 容量瓶中,用纯水定容,得 $0.010\ \text{mol/L}$ 硝酸铀酰溶液。于 $500\ \text{mL}$ 容量瓶中加入适量硝酸铀酰溶液,再加入适量酒石酸溶液,用纯水定容,即得一系列酒石酸铀酰样品溶液,待 ESI-MS/MS 分析。

## 2 结果与讨论

### 2.1 酒石酸铀酰溶液中铀酰形态分析

向酒石酸中加入硝酸铀酰溶液后产生多种酒石酸铀酰络合物离子,其全扫描质谱图示于图 1。传统质谱分析方法需在鉴别化合物结构

后才能确定其是否含铀,工作量大、分析效率低。含铀化合物的本质特点是其分子结构中存在铀酰基团( $[\text{UO}_2]^+$ , $m/z 269.9$ ),因此本研究采用质谱高碰撞能量轰击目标物,产生铀酰离子信号的离子即为含铀化合物。通过这种方法确定了溶液中的含铀离子,鉴定出 5 种无机铀酰和 14 种酒石酸铀酰形态,列于表 1。该结果既表明了铀络合形态的多样性和复杂性,也验证了电喷雾串联质谱研究水溶液中铀络合形态的优势。其中  $m/z 1\ 121.3$ 、 $m/z 460.1$  等低响应、多电荷或结构未能解析的离子,在 $200\ \text{V}$ 高碰撞能量下均只存在唯一的 $[\text{UO}_2]^+$ 离子信号,结果示于图 2。

### 2.2 酒石酸与铀酰络合形态质谱解析

**2.2.1 单酒石酸铀酰形态的结构表征及质谱裂解途径** 1 个酒石酸阴离子与 1 个铀酰基团结合形成带 1 个正电荷的络合物离子  $m/z 418.9$ 。CID 为 $5\ \text{V}$  时, $[\text{UO}_2\text{HTar}]^+$ 失去 1 个 $\cdot\text{COOH}$  基团,与脱去 1 个 $\cdot\text{H}$  的邻位碳结合形成双键,产生较弱响应的  $m/z 373.0$ 。另外, $[\text{UO}_2\text{HTar}]^+$  可失去 2 个 $\cdot\text{COOH}$  基团,2 个连接羧基的碳原子结合形成碳碳双键,产生响应值较高的  $m/z 328.9$ , $m/z 328.9$  还可进一步失去 1 个 $\cdot\text{CH}$  产生  $m/z 300.9$ 。当 CID 增大至 $50\ \text{V}$  时,产生明显的 $[\text{UO}_2]^+$ 信号,示于图 3, $[\text{UO}_2\text{HTar}]^+$  的质谱裂解途径示于图 4。 $m/z 328.9$  的结构表明,酒石酸分子是通过羟基上的氧原子而非羧基上的氧原子与铀酰络

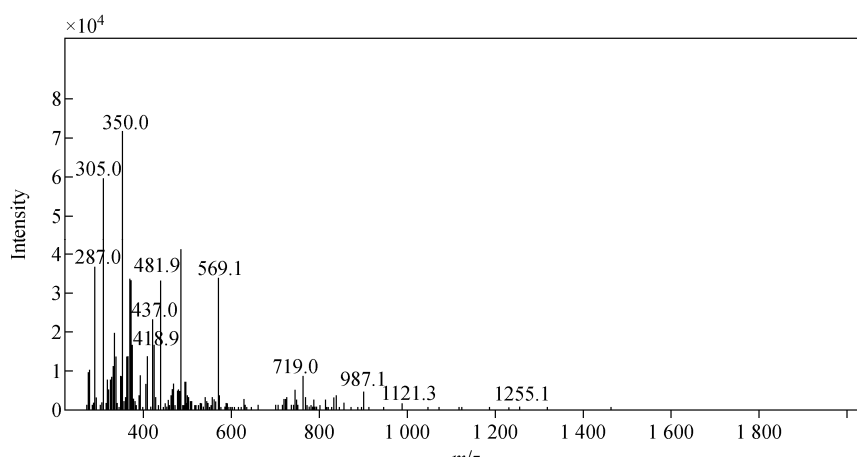


图 1 酒石酸铀酰溶液的全扫描质谱图

Fig. 1 Full scan mass spectrum of uranyl tartrate solution

表 1 酒石酸与硝酸铀酰溶液中的铀形态

Table 1 Uranium speciation of tartaric acid and uranyl nitrate complex in solution

质荷比 <i>m/z</i>	结构式 Structural formula	质荷比 <i>m/z</i>	结构式 Structural formula
1255.1	—	481.9	$[\text{UO}_2 \text{HTarHNO}_3]^+$
1121.3	—	460.1	—
987.1	—	437.0	$[\text{UO}_2 \text{HTarH}_2\text{O}]^+$
837.1	—	418.9	$[\text{UO}_2 \text{HTar}]^+$
778.1	$[(\text{UO}_2)_3 \text{Tar}(\text{HTar})_2(\text{H}_2\text{Tar})_2]^{2+}$	350.0	$[\text{UO}_2 \text{NO}_3 \text{H}_2\text{O}]^+$
719.1	$[\text{UO}_2 \text{HTar}(\text{H}_2\text{Tar})_2]^+$	332.0	$[\text{UO}_2 \text{NO}_3]^+$
703.1	$[(\text{UO}_2)_3 \text{Tar}(\text{HTar})_2]^{2+}$	322.9	$[\text{UO}_2 \text{H}_2\text{OOH}]^+$
587.1	$[\text{UO}_2 \text{HTarH}_2\text{TarH}_2\text{O}]^+$	305.0	$[\text{UO}_2 \text{H}_2\text{OOH}]^+$
569.1	$[\text{UO}_2 \text{HTarH}_2\text{Tar}]^+$	287.0	$[\text{UO}_2 \text{OH}]^+$
569.1	$[(\text{UO}_2 \text{HTarH}_2\text{Tar})_2]^{2+}$		

注：“—”表示结构未知

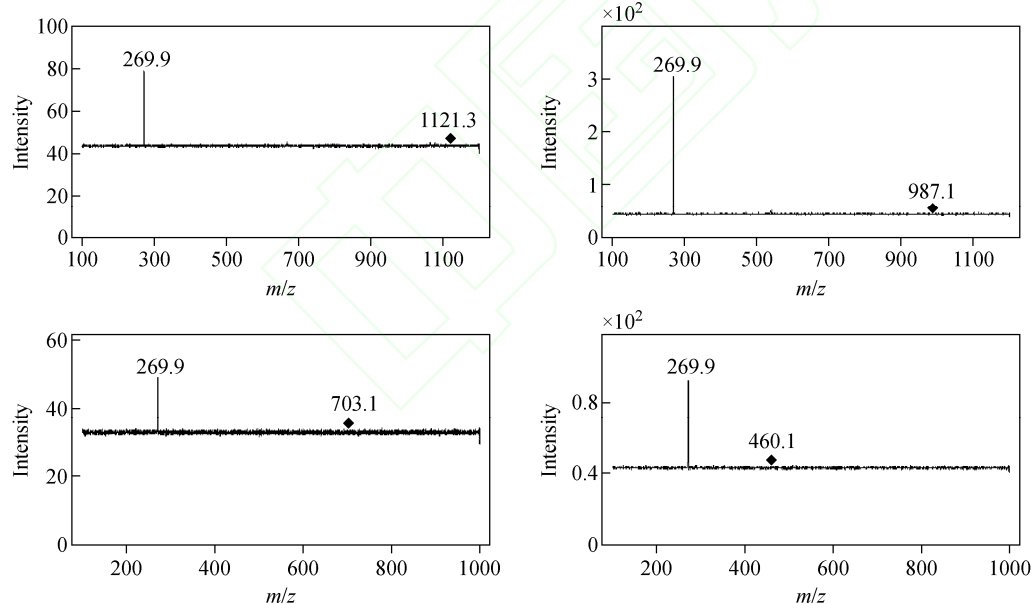


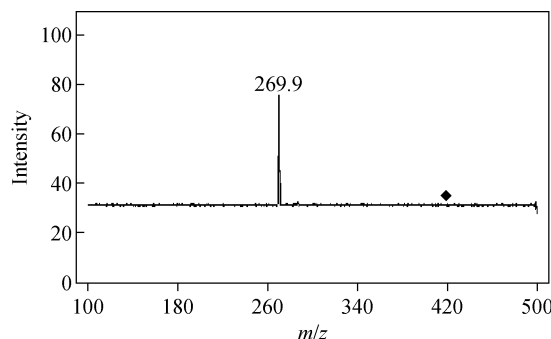
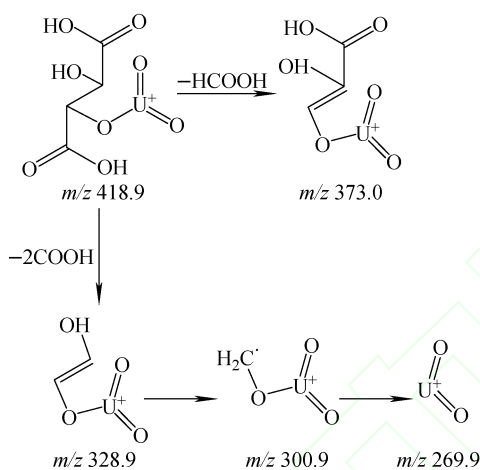
图 2 高质谱碰撞能量鉴别含铀离子的质谱图(CID 200 V)

Fig. 2 Mass spectra of identification of uranium ions by high mass spectrometry collision energy (CID 200 V)

合。酒石酸铀酰一聚物还可结合 1 个水分子或硝酸分子形成  $[\text{UO}_2 \text{HTarH}_2\text{O}]^+$  (*m/z* 437.0) 或  $[\text{UO}_2 \text{HTarHNO}_3]^+$  (*m/z* 481.9)。

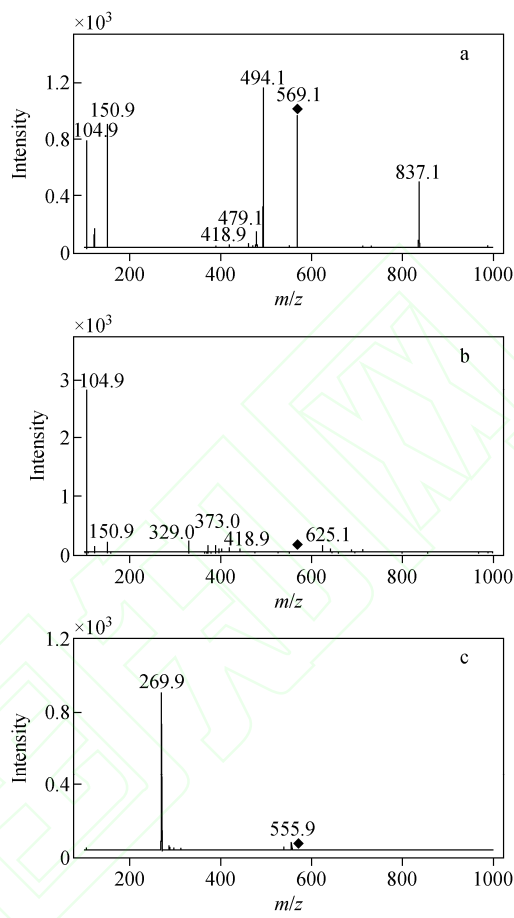
**2.2.2 多聚酒石酸铀酰团簇的结构表征及质谱裂解途径** *m/z* 569.1 存在单电荷离子与双电荷离子的质谱信号。当碰撞能量为 5 V 时, 产生明显的酒石酸阳离子 *m/z* 150.9 及其脱 $\cdot\text{COOH}$ 的子离子 *m/z* 104.9, 同时 *m/z* 569.1

失去 *m/z* 75 形成显著的 *m/z* 494.1 子离子, 示于图 5a。*m/z* 569.1 主要以双电荷离子  $[(\text{UO}_2 \text{HTarH}_2\text{Tar})_2]^{2+}$  形态存在, 该离子容易丢失 2 个酒石酸分子产生较强响应的 *m/z* 837.1( $[(\text{UO}_2)_2 \text{TarHTar}]^+$ ), 其裂解途径示于图 6a。该结果表明, 以分子形式络合的酒石酸与铀酰的结合较弱。由于共轭双键的稳定作用, 单电荷离子  $[\text{UO}_2 \text{HTarH}_2\text{Tar}]^+$  可脱去 2

图 3  $[\text{UO}_2\text{HTar}]^+$  子离子扫描质谱图 (CID 50 V)Fig. 3 Product ions scan mass spectrum of  $[\text{UO}_2\text{HTar}]^+$  (CID 50 V)图 4  $[\text{UO}_2\text{HTar}]^+$  质谱裂解途径Fig. 4 MS fragmentation pathways of  $[\text{UO}_2\text{HTar}]^+$ 

个 $\cdot\text{COOH}$ 形成特征离子  $m/z\ 479.1$ ,其质谱裂解途径示于图 6b。当碰撞能量提高至 20 V,  $m/z\ 569.1$  可形成失去羧基、水的离子  $m/z\ 625.1$ 、 $418.9$ 、 $373.0$ 、 $329.0$ ,结果示于图 5b。继续提高碰撞能量至 80 V,  $[(\text{UO}_2\text{HTarH}_2\text{Tar})_2]^{2+}$  产生显著的  $[\text{UO}_2]^+$  信号,以及微弱的  $m/z\ 555.9$ ,示于图 5c。该结果表明,双铀酰聚合离子具有较强的质谱稳定性,其解离能量大于酒石酸阴离子的官能团解离所需的能量。

$m/z\ 719.1$  ( $[\text{UO}_2\text{HTar}(\text{H}_2\text{Tar})_2]^{2+}$ ) 为铀酰基团结合 1 个酒石酸阴离子和 2 个酒石酸分子形成的离子。与  $m/z\ 569.1$  不同,  $m/z\ 719.1$  不产生大于自身的子离子,也检测不到酒石酸阳离子或其碎片离子信号,这表明  $m/z\ 719.1$  为单电荷阳离子。 $[\text{UO}_2\text{HTar}(\text{H}_2\text{Tar})_2]^{2+}$

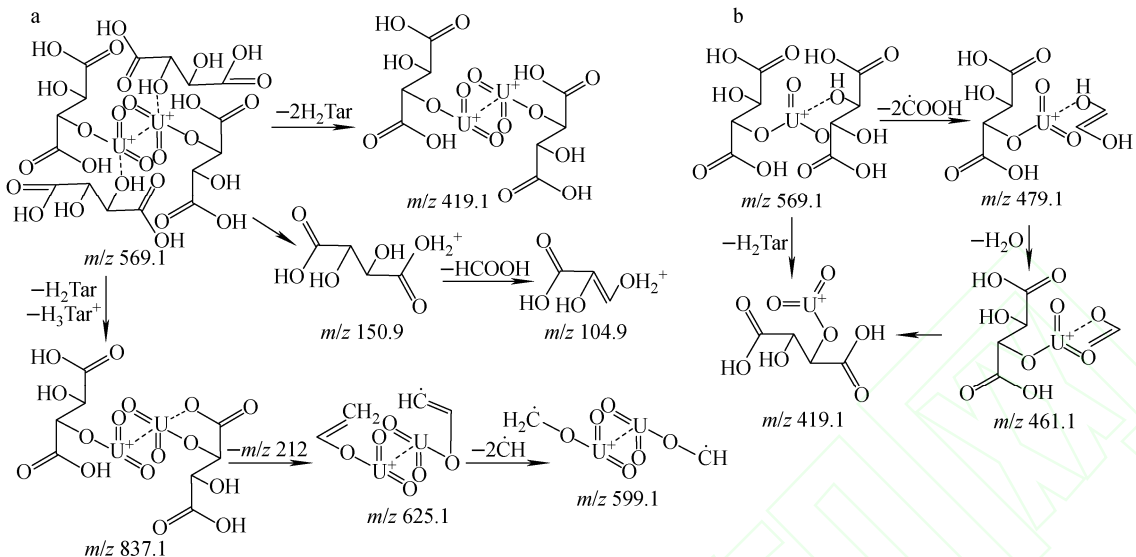
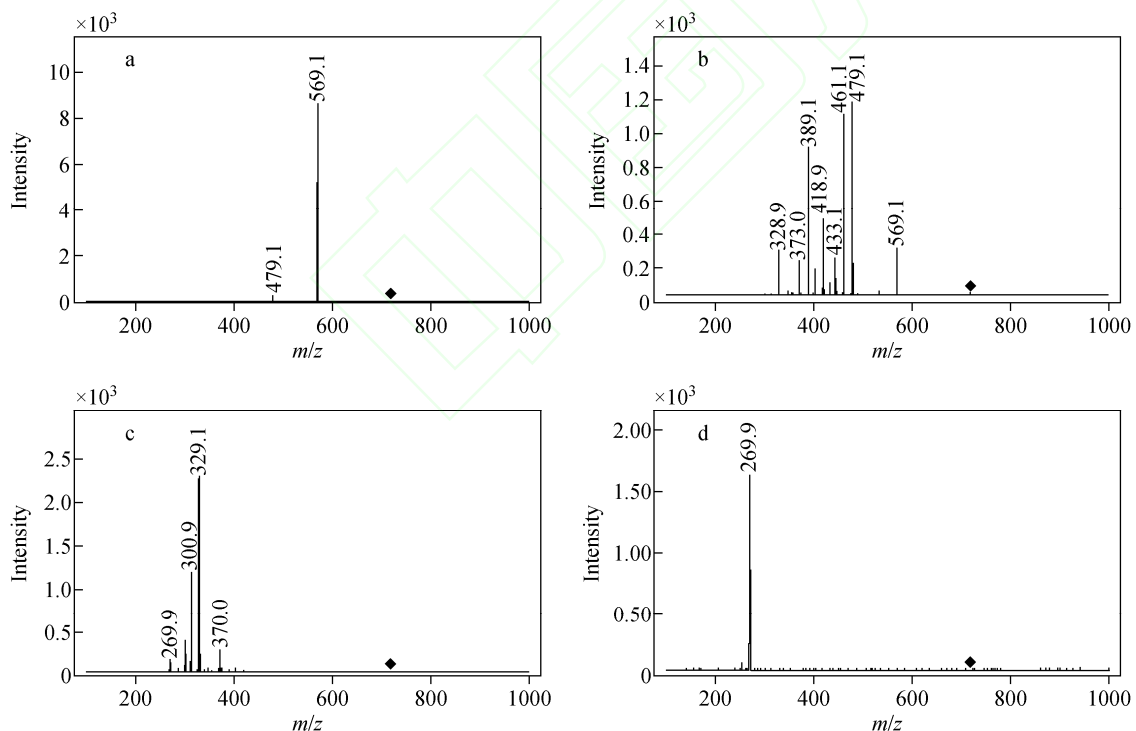


注:a. CID 为 5 V; b. CID 为 20 V; c. CID 为 80 V

图 5  $m/z\ 569.1$  的子离子扫描质谱图Fig. 5 Product ions scan mass spectrum of  $m/z\ 569.1$ 

被 10 V 能量轰击,脱去 1 个酒石酸分子产生  $[\text{UO}_2\text{HTarH}_2\text{Tar}]^+$  子离子,示于图 7a。增大碰撞能量至 25 V,出现  $m/z\ 479.1$ 、 $461.1$ 、 $418.9$  等碎片离子,示于图 7b。继续提高 CID 至 50 V 时,主要的子离子为  $m/z\ 370.0$ 、 $329.1$ 、 $300.9$  等  $[\text{UO}_2\text{HTar}]^+$  碎片离子和  $[\text{UO}_2]^+$  信号,示于图 7c。当 CID 为 200 V 时, $[\text{UO}_2\text{HTar}(\text{H}_2\text{Tar})_2]^{2+}$  产生明显的  $[\text{UO}_2]^+$  信号,示于图 7d。 $[\text{UO}_2\text{HTar}(\text{H}_2\text{Tar})_2]^{2+}$  的质谱裂解途径示于图 8。

$m/z\ 778.1$  ( $[(\text{UO}_2)_3\text{Tar}(\text{HTar})_2(\text{H}_2\text{Tar})_2]^{2+}$ ) 也是双电荷酒石酸铀酰离子,它通过两种途径裂解:1) 三铀酰聚合离子  $[(\text{UO}_2)_3\text{Tar}(\text{HTar})_2(\text{H}_2\text{Tar})_2]^{2+}$  被低能量碰撞后,失去 1 个酒石酸分子和 1 个酒石酸阳离子,产生单电荷阳离子  $m/z\ 1255.1$  信号;2)  $m/z\ 778.1$  逐渐失去 2

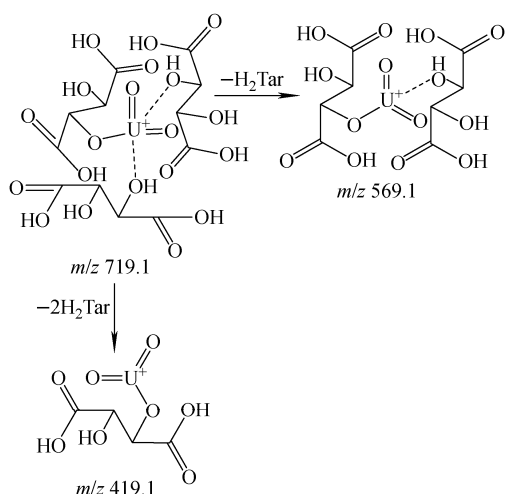
图 6  $m/z$  569.1 的质谱裂解途径Fig. 6 MS fragmentation pathways of  $m/z$  569.1

注:a. CID 为 10 V;b. CID 为 25 V;c. CID 为 50 V;d. CID 为 200 V

图 7  $[\text{UO}_2\text{HTar}(\text{H}_2\text{Tar})_2]^{2+}$  的子离子扫描质谱图Fig. 7 Product ions scan mass spectra of  $[\text{UO}_2\text{HTar}(\text{H}_2\text{Tar})_2]^{2+}$ 

个酒石酸分子,产生  $m/z$  703.1、628.1 信号。由于共轭双键的作用, $[(\text{UO}_2)_3\text{Tar}(\text{HTar})_2(\text{H}_2\text{Tar})_2]^{2+}$  在较高碰撞能量下,结合的多聚铀酰离子分离形成一系列复杂的离子碎片,这些

多聚铀酰离子的质谱稳定性较强,不易产生单铀酰离子。在 200 V 碰撞能量下, $[(\text{UO}_2)_3\text{Tar}(\text{HTar})_2(\text{H}_2\text{Tar})_2]^{2+}$  产生明显的 $[\text{UO}_2]^{2+}$  信号。不同碰撞能量下, $[(\text{UO}_2)_3\text{Tar}(\text{HTar})_2(\text{H}_2\text{Tar})_2]^{2+}$

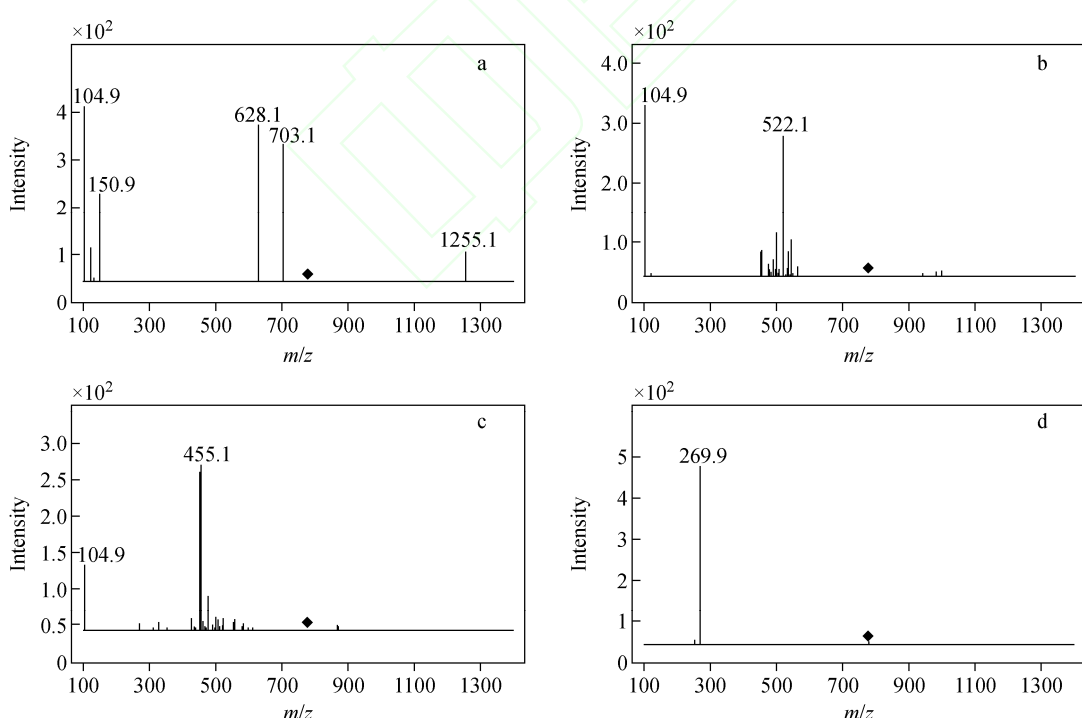
图 8  $[\text{UO}_2\text{HTar}(\text{H}_2\text{Tar})_2]^+$  的质谱裂解途径Fig. 8 MS spectral fragmentation pathways  
of  $[\text{UO}_2\text{HTar}(\text{H}_2\text{Tar})_2]^+$ 

的子离子扫描质谱图示于图 9,其裂解途径示于图 10。本实验中,因  $m/z$  987.1、1 121.3 响应值太低或超出本仪器扫描范围,故暂未分析

其结构。

### 3 结论

本研究以电喷雾串联质谱研究酒石酸-硝酸铀酰水溶液中的铀酰形态,以  $[\text{UO}_2]^+$  为鉴别含铀离子的依据,共发现 14 种酒石酸铀酰络合物及 5 种无机铀酰形态。酒石酸铀酰形态中铀酰与酒石酸阴离子结合紧密,还可继续结合 1~2 个酒石酸或水分子,形成二铀酰、三铀酰聚合的酒石酸铀酰络合物,其中  $[\text{UO}_2\text{HTar}(\text{H}_2\text{Tar})_2]^+$  等多聚酒石酸铀酰团簇形态为首次发现。酒石酸铀酰形态中各络合键解离所需能量大小顺序为:铀酰间结合键>酒石酸阴离子-铀酰结合键>酒石酸分子-铀酰结合键。电喷雾串联质谱法无需样品前处理,不改变溶液原有形态,在水溶液含铀形态分析中具有独特优势,可为实际条件下核素与有机酸的水溶液形态研究提供数据和方法支持。



注:a. CID 为 10 V;b. CID 为 35 V;c. CID 为 50 V;d. CID 为 200 V

图 9  $[(\text{UO}_2)_3\text{Tar}(\text{HTar})_2(\text{H}_2\text{Tar})_2]^{2+}$  的子离子扫描质谱图Fig. 9 Product ions scan mass spectra of  $[(\text{UO}_2)_3\text{Tar}(\text{HTar})_2(\text{H}_2\text{Tar})_2]^{2+}$

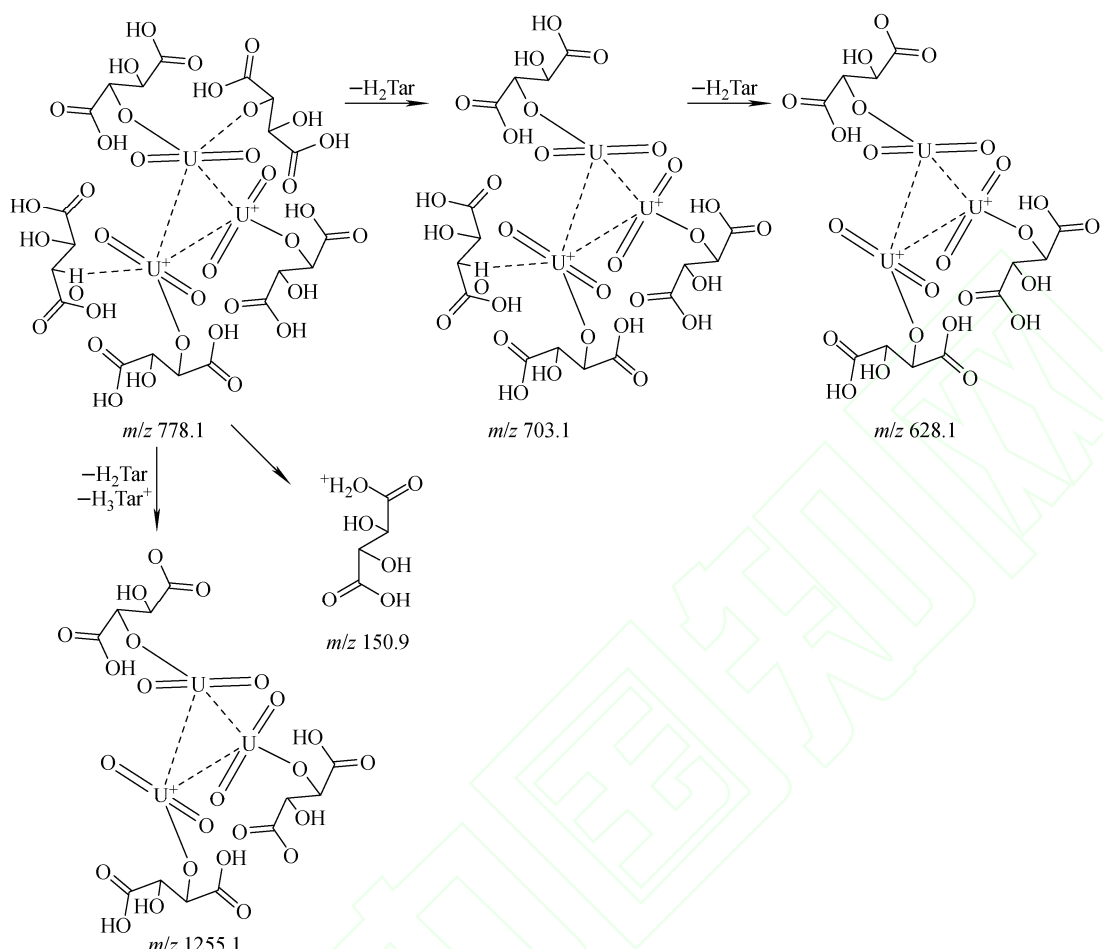


图 10  $[(\text{UO}_2)_3 \text{Tar}(\text{HTar})_2 (\text{H}_2\text{Tar})_2]^{2+}$  的质谱裂解途径

Fig. 10 MS fragmentation pathways of  $[(\text{UO}_2)_3 \text{Tar}(\text{HTar})_2 (\text{H}_2\text{Tar})_2]^{2+}$

## 参考文献：

- [1] MONTELONGO M, HERRERA E, RAMIREZ E, CARRILLO J, CAMPOS A, GOMEZ R, MONTERO M, RODRIGUEZ L. Study of radioactive contamination in silts and aerosols at Al-dama city, Mexico, due to the operation of a yellow-cake processing plant[J]. Journal of the Air & Waste Management Association, 2015, 65 (8): 895-902.
- [2] FAVAS P, PRATAS J, MITRA S, SARKAR S, VENKATACHALAM P. Biogeochemistry of uranium in the soil-plant and water-plant systems in an old uranium mine[J]. Science of the Total Environment, 2016, 568: 350-368.
- [3] 张学礼,徐乐昌,张辉.某铀尾矿库周围农田土壤重金属污染潜在生态风险评价[J].中国环境监测,2016,32(6):76-83.
- ZHANG Xueli, XU Lechang, ZHANG Hui. Potential ecological risk assessment of heavy metals contamination in farmland soils near an uranium tailings pond[J]. Environmental Monitoring in China, 2016, 32(6): 76-83(in Chinese).
- [4] RUEDIG E, JOHNSON T. An evaluation of health risk to the public as a consequence of in situ uranium mining in Wyoming, USA[J]. Journal of Environmental Radioactivity, 2015, 150: 170-178.
- [5] 郭永海,王海龙,董建楠,刘淑芬,苏锐,宗自华.高放废物处置库野马泉预选地段地下水铀存在形式及迁移特征[J].原子能科学技术,2012,46 (S1):79-83.
- GUO Yonghai, WANG Hailong, DONG Jian-nan, LIU Shufen, SU Rui, ZONG Zihua. Uranium occurrence species and migration features of groundwater in yemaquan preselected section for China's HLW disposal repositroy[J]. Atomic

- Energy Science and Technology, 2012, 46(S1): 79-83(in Chinese).
- [6] 赖捷, 阳刚, 冷阳春, 庚先国. 铀在西南某废物处置库土壤中的吸附迁移规律[J]. 西南科技大学学报, 2017, 32(3): 1-7.
- LAI Jie, YANG Gang, LENG Yangchun, TUO Xianguo. Research on adsorption and migration patterns of uranium in the waste repository soil in the southwest[J]. Journal of Southwest University of Science and Technology, 2017, 32(3): 1-7(in Chinese).
- [7] 司高华, 李哲, 宣宝峰. 超铀核素在某处置工程地下水化学形态分析研究[J]. 地下水, 2017, 39(1): 24-26.
- SI Gaohua, LI Zhe, XUAN Baofeng. The calculation of transuranic radionuclides forms in ground water of a disposal engineering[J]. Ground Water, 2017, 39 (1): 24-26 (in Chinese).
- [8] KRAWCZYK-BRÄSCH E, LÜTKE L, MOLL H, BOK F, STEUDTNER R, ROSSBERG A. A spectroscopic study on U(VI) biomimetication in cultivated *pseudomonas fluorescens* biofilms isolated from granitic aquifers[J]. Environmental Science and Pollution Research, 2015, 22 (6): 4 555-4 565.
- [9] HOLMES A, JOYCE K, XIE H, FALANK C, HINZ J, WISE J. The impact of homologous recombination repair deficiency on depleted uranium elastogenicity in Chinese hamster ovary cells: XRCC3 protects cells from chromosome aberrations, but increases chromosome fragmentation [J]. Mutation Research/ Fundamental and Molecular Mechanisms of Mutagenesis, 2014, 762: 1-9.
- [10] FATHI R, MATTI L, AL-SALIH H, GOODBOLD D. Environmental pollution by depleted uranium in Iraq with special reference to Mosul and possible effects on cancer and birth defect rates[J]. Medicine Conflict & Survival, 2013, 29(1): 7-25.
- [11] PATTISON J. The interaction of natural background gamma radiation with depleted uranium micro-particles in the human body[J]. Journal of Radiological Protection, 2013, 33(1): 187-198.
- [12] PANNU T, SUKHMAMI, GILL K. Uranium-toxicity and uranium-induced osteosarcoma using a new regimen and surgery: a first-time experience[J]. Journal of Clinical and Diagnostic Research, 2015, 9(6): 1-3.
- [13] 潘自强, 钱七虎. 高放废物地质处置战略研究[M]. 北京: 原子能出版社, 2009: 279-312.
- [14] JHA V, TRIPATHI R, SETHY N, SAHOO S. Uptake of uranium by aquatic plants growing in fresh water ecosystem around uranium mill tailings pond at Jaduguda, India[J]. Science of the Total Environment, 2016, 539: 175-184.
- [15] ZHAO C, LI X, DING C, LIAO J, DU L, YANG J, YANG Y, ZHANG D, TANG J, LIU N, SUN Q. Characterization of uranium bioaccumulation on a fungal isolate *geotrichum sp. dwc-1* as investigated by FTIR, TEM and XPS[J]. Journal of Radioanalytical and Nuclear Chemistry. 2016, 310(1): 1-11.
- [16] YI Z, YAO J, CHEN H, WANG F, YUAN Z, LIU X. Uranium biosorption from aqueous solution onto *Eichhornia Crassipes* [J]. Journal of Environmental Radioactivity, 2016, 154: 43-51.
- [17] NIE X, DONG F, LIU N, LIU M, ZHANG D, KANG W, SUN S, ZHANG W, YANG J. Subcellular distribution of uranium in the roots of *Spirodela punctata* and surface interactions[J]. Applied Surface Science, 2015, 347: 122-130.
- [18] AL-HAMARNEH I, ALKHOMASHI N, ALMASOUD F, ALMASOUD I. Study on the radioactivity and soil-to-plant transfer factor of  $^{226}\text{Ra}$ ,  $^{234}\text{U}$  and  $^{238}\text{U}$  radionuclides in irrigated farms from the northwestern Saudi Arabia[J]. Journal of Environmental Radioactivity, 2016, 160: 1-7.
- [19] PATERSON-BEEDLE M, READMAN J, HRILJAC J, MACASKIE L. Biorecovery of uranium from aqueous solutions at the expense of phytic acid[J]. Hydrometallurgy, 2010, 104(3/4): 524-528.
- [20] SANTSCHI P, ROBERTS K, GUO L. Organic nature of colloidal actinides transported in surface water environments[J]. Environmental Science & Technology, 2002, 36(17): 3 711-3 719.
- [21] CANON F, PATÉ F, MEUDEC E, MARLIN T, CHEYNIER V, GIULIANI A, SARINI-MANCHADO P. Characterization, stoichiometry, and stability of salivary protein-tannin complexes by ESI-MS and ESI-MS/MS[J]. Analyti-

- cal & Bioanalytical Chemistry, 2009, 395: 2 535-2 545.
- [22] PASILIS S, PEMBERTON J. Speciation and coordination chemistry of uranyl(Ⅵ)-citrate complexes in aqueous solution[J]. Inorganic Chemistry, 2003, 42(21): 6 793-6 800.
- [23] TSERKEZOS N, ROITHOVÁ J, SCHRÖDER D, ONČÁK M, SLAVIČEK. Can electrospray mass spectrometry quantitatively probe speciation hydrolysis of uranyl nitrate studied by gas-phase methods[J]. Inorganic Chemistry, 2009, 48 (13): 6 287-6 296.
- [24] GATHERINE C, NERO M. Trace level uranyl complexation with phenylphosphonic acid in aqueous solution direct speciation by high resolution mass spectrometry[J]. Inorganic Chemistry, 2013, 52: 4 372-4 383.
- [25] THUÉRY P. Uranyl ion complexation by citric and citramalic acids in the presence[J]. Inorganic Chemistry, 2007, 46: 2 307-2 315.
- [26] LUO M, HU B, ZHANG X, PENG D, CHEN H, ZHANG L, HUAN Y. Extractive electrospray ionization mass spectrometry for sensitive detection of uranyl species in natural water samples[J]. Analytical Chemistry, 2010, 82 (1): 282-289.
- [27] SHELLEY J, BADAL S, ENGELHARD C, HAYEN H. Ambient desorption/ionization mass spectrometry: evolution from rapid qualitative screening to accurate quantification tool[J]. Analytical & Bioanalytical, 2018, 410 (17): 4 061-4 076.
- [28] 胡斌, 陈焕文, 张燮, 杨水平, 冯守华. 新化合物五氧化铀的电喷雾串联质谱法制备与表征[J]. 化学学报, 2009, 67(12): 1 331-1 335.  
HU Bin, CHEN Huanwen, ZHANG Xie, YANG Shuiping, FENG Shouhua. Preparation and characterization of UO<sub>5</sub> by using electrospray ionization tandem mass spectrometry[J]. Acta Chimica Sinica, 2009, 67(12): 1 331-1 335 (in Chinese).
- [29] LI Y, YANG M, SUN R, ZHONG T, CHEN H. Detection of uranium in industrial and mines samples by microwave plasma torchmass spectrometry[J]. Journal of Mass Spectrometry, 2016, 51(2): 159-164.
- [30] DAVIS A L, CLOWERS B H. Stabilization of gas-phase uranyl complexes enables rapid speciation using electrospray ionization and ion mobility-mass spectrometry[J]. Talanta, 2018, 176: 140-150.